2011 International Symposium on Nonlinear Theory and its Applications
NOLTA2011, Kobe, Japan, September 4-7, 2011

Local cortical design of voltage-based STDP

Hideyuki Kato[†,§] and Tohru Ikeguchi[†,‡,¶]

[†] Graduate School of Science and Engineering, Saitama University
[‡] Saitama University, Brain Science Institute
255 Shimo-okubo, Sakura-ku, Saitama-city, Saitama, 338-8570
Email: [§]hide@ifisc.uib-csic.es, [¶]tohru@mail.saitama-u.ac.jp

Abstract— In this study we investigated properties of a voltage-based spike timing-dependent plasticity (STDP) model, that is based on the presynaptic firings and the postsynaptic membrane potential, by performing network motif extraction. We compared results obtained by a standard STDP model, in which synapses change depending only on timing of pre- and postsynaptic firings. As a result, the voltage-based STDP can induce strong bidirectional connections not only between two neurons but also among three neurons. These results relate to localization of strong feedforward connections. Our results suggest that the voltage-based STDP model may realize the statistics of synapses observed in cortical circuits.

1. Introduction

It has been generally believed that synaptic plasticity plays an important role to accomplish higher-brain functions such as memory, learning, and development since Hebb's postulation [1]. To maintain neuronal activity and process information, synapses in the brain dynamically change their weights depending on neuronal activities.

STDP is one of the synaptic modification principles in the brain [2, 3]. In standard phenomenological models of STDP, synaptic modifications are triggered only by precise timing between pre- and postsynaptic spikes [4–6]. However, recent studies show that STDP depends not only on precise timing between pre- and postsynaptic spikes but also on frequency of pairing protocols, cooperativity of synapses, and the postsynaptic membrane potential [7].

Although many of bidirectional connections in the cortices have significantly strong weights [8, 9], the standard phenomenological STDP models cannot realize strong bidirectional connections, that is, one connection between two neurons is depressed if another connection is potentiated [10]. In contrast to the standard models, a novel phenomenological STDP model, which introduces the postsynaptic membrane potential, can potentiate bidirectional synaptic connections [11]. In Ref. [11], the connectivity between two neurons was discussed. In Refs. [8, 9], it was shown that bidirectional connections in cortical circuits are more clustered compared with random networks, then bidirectional connections among three neurons are also stronger than unidirectional connections. It is natural to consider that such strong bidirectional connections might be organized by STDP. Such clustering of strong bidirectional synaptic connection should contribute to the presence of the third-order correlations [12, 13]. Then, it is very important to analyze the connectivity among three neurons because the model of third-order correlations fits experimental data much better than that of pair-wise correlations.

Accordingly, we investigated properties of the voltage-based STDP model with respect to bidirectional connections by analyzing connectivity patterns called network motifs [14]. Our result showed that the voltage-based model got much more strong bidirectional connections than the standard model.

2. Materials and Methods

The dynamics of a single neuron model in our network is written in the differential equations,

$$\begin{aligned} \frac{d}{dt}v &= 0.04v^2 + 5v + 140 - u + I(t), \\ \frac{d}{dt}u &= a(bv - u), \end{aligned} \tag{1}$$

where v and u were the membrane potential and the recovery variable of the neuron [15]. v and u were reset to c and $u + d$ if v reached 30 mV. In this neuron model, a, b, c, and d were parameters. A synaptic current into a neuron was described as $I(t) = -g_{\mathrm{ex}}(v - E_{\mathrm{ex}}) - g_{\mathrm{inh}}(v - E_{\mathrm{inh}})$, where E_{ex} and E_{inh} were reversal potentials. The kinetics of a synaptic conductance g_{ex}, obeyed the equation of $\tau\dot{g} = -g$ with a time constant τ_{ex}, when synaptic inputs were absent. In contrast to the absence of inputs, an arrival of a spike at an excitatory synapse increased g_{ex} by $\overline{g}_i^{\mathrm{rec}}$. The variable g_{inh} also obeyed the same manner, but the unit of the increment was $\overline{g}_{\mathrm{inh}}$ and a time constant was τ_{inh}. Both $\overline{g}_i^{\mathrm{rec}}$ and $\overline{g}_{\mathrm{inh}}$ represented the peak synaptic conductances.

Our network consisted of forty excitatory (regular spiking) neurons and ten inhibitory (fast spiking) neurons. The parameters for excitatory and inhibitory neurons in the neuron model were referred to Ref. [15]. The excitatory neurons in the network had all-to-all connectivity before learning. Each excitatory neuron received seven connections from randomly selected inhibitory neurons and projected back to eight inhibitory neurons.

In addition to the recurrent connections, each neuron received inputs from 500 excitatory Poisson neurons through feedforward connections. The circular boundary condition was assumed, namely, the neuron 500 was next to the neuron 1. The firing rates ρ_i^{pre} of these neurons were characterized by the Gaussian profile $\rho_i^{\mathrm{pre}} = \alpha \exp\left(\frac{-(i-\mu)^2}{2\sigma^2}\right)$, where α was the firing rate of a center neuron, and μ was the index of the center neuron. The center index of μ was shifted at every $\mathcal{T}$ ms. The peak conductance of a feedforward synaptic connection was $\overline{g}_i^{\mathrm{ff}}$, and an arrival of a spike at a synaptic terminal increased g_{ex} by $\overline{g}_i^{\mathrm{ff}}$.

Synapses between excitatory neurons were continuously modified by the voltage-based STDP [11]. The changes of the synapse i on a neuron were

$$\frac{d}{dt}\overline{g}_i = -A_-(\overline{\overline{u}})X_i(t)(\overline{u}_- - \theta_-)_+ + A_+\overline{x}_i(v-\theta_+)_+(\overline{u}_+ - \theta_-)_+. \quad (2)$$

The variable $\overline{u}_-$ was low-pass-filtered membrane potential with a time constant τ_-, and behaved as

$$\tau_- \frac{d}{dt}\overline{u}_-(t) = -\overline{u}_-(t) + v(t). \quad (3)$$

The variable $\overline{u}_+$ had the same form as Eq. (3) but had a different time constant τ_+. The trace of presynaptic spikes $\overline{x}_i$ was written by

$$\tau_x \frac{d}{dt}\overline{x}_i(t) = -\overline{x}_i(t) + X_i(t), \quad (4)$$

where $X_i(t) = \sum_n \delta(t - t_i^n)$ represented a presynaptic spike sequence. Here t_i^n was the arrival time of the nth spike at the synapse i. In Eq. (2), A_+ was the amplitude of long-term potentiation (LTP), while $A_-(\overline{\overline{u}}) = A_-\frac{\overline{\overline{u}}^2}{u_{\mathrm{ref}}^2}$ was for long-term depression (LTD). The amplitude of LTD varied depending on the value $\overline{\overline{u}}$, which corresponded to the averaged value of $\overline{u}_-$ of the postsynaptic neuron. $\overline{u}_-$ was averaged for 1 s in accordance with Ref. [11]. Synaptic weights were constrained with hardbounds. The lower bounds of both $\overline{g}_i^{\mathrm{rec}}$ and $\overline{g}_i^{\mathrm{ff}}$ were zero, whereas the upper bound of $\overline{g}_i^{\mathrm{rec}}$ was different from that of $\overline{g}_i^{\mathrm{ff}}$. Their maximum values were respectively described by $\overline{g}_{\mathrm{max}}^{\mathrm{rec}}$ and $\overline{g}_{\mathrm{max}}^{\mathrm{ff}}$.

In addition to the voltage-based model, we also simulated a neural network with a standard STDP model [4]. The dynamics of synaptic weights in the standard STDP rule depended only on pre- and postsynaptic spikes, and was expressed as

$$\frac{d}{dt}\overline{g}_i = -A_d X_i(t)\overline{y}(t) + A_p Y(t)\overline{x}_i(t), \quad (5)$$

where $Y(t)$ and $\overline{y}(t)$ were respectively the same as $X_i(t)$ and $\overline{x}_i(t)$, but for a postsynaptic neuron. A time constant for $\overline{y}(t)$ and $\overline{x}_i(t)$ in Eq. (5) was τ. A_d and A_p were parameters that determined synaptic changes when an interval of pre- and postsynaptic spikes was close to zero.

In this study, we analyzed connectivity among excitatory neurons in the recurrent network. We used local connectivity patterns called network motifs [14] to analyzed the connectivity. We performed the network motif extraction with a fast detection algorithm [16]. When we extracted the network motifs, we considered only synapses, that exceeded a threshold $g_\theta = \frac{2}{3}\overline{g}_{\mathrm{max}}^{\mathrm{rec}}$ in the recurrent network.

All the parameters are concluded in Table 1. The learning rates of Eq. (5) was set to different values from those of Eq. (2) to make the amounts of synaptic changes of Eq. (5) comparable with those of Eq. (2). It was impossible that the amounts of synaptic changes of Eq. (2) was completely matched to those of Eq. (5) because synaptic changes of Eq. (2) varied depending on postsynaptic neuronal states. In other words, although the learning rates of Eq. (2) was much smaller than those of Eq. (5), values of membrane potential also contributed to synaptic changes in Eq. (2). Then the differences of the learning rates filled the gap of synaptic changes between Eqs. (2) and (5) during learning. A schematic diagram of our experiments is depicted in Fig. 1.

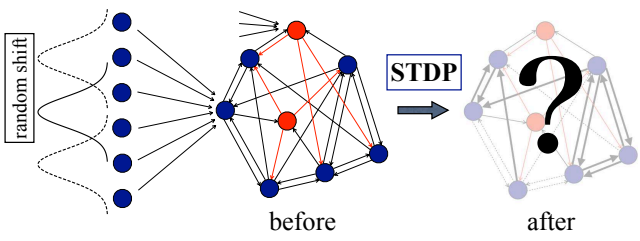

Figure 1: A schematic diagram of our experiment. Red and blue nodes represent inhibitory and excitatory neurons. Red and black arrows are inhibitory and excitatory synaptic connections.

3. Results

After learning with a standard STDP model, almost all the synapses in the recurrent network are unidirectional even if the duration are varied, whereas much fewer unidirectional connections are strengthened by the voltage-based STDP (Fig. 2A, ID 1). In contrast to unidirectional connections, the tendency of bidirectional connections is opposite (Fig. 2A, ID 2). The voltage-based STDP frequently strengthens bidirectional connections in the recurrent network. These results are consistent with the results of Ref. [11].

This tendency is also inherited to three-neuron connectivity patterns. All the connectivity patterns composed of only unidirectional connections are frequently observed af-

Table 1: Parameters of the model.

Parameters	Values
E_{ex}	0 mV
E_{inh}	−70 mV
τ_{ex}	5 ms
τ_{inh}	7 ms
$\overline{g}^{\mathrm{rec}}$	$0.0036^{*,**}$, 0.06^{***}
$\overline{g}_{\mathrm{inh}}$	0.08
α	30 Hz
σ	10
$\overline{g}^{\mathrm{ff}}$	$[0.0071, 0.0281]^{*,**}$, 0.05^{***}
A_-	2.0×10^{-6}
A_+	1.14×10^{-6}
u_{ref}^2	60 mV^2
τ_-	10 ms
τ_+	7 ms
τ_x	15 ms
$\overline{g}_{\mathrm{max}}^{\mathrm{rec}}$	0.011
A_d	0.002
A_p	0.0021
τ	20 ms

* means initial values before learning but these values change according to STDP. ** indicates an excitatory synaptic conductance on excitatory neurons, and *** indicates an excitatory synaptic conductance on inhibitory neurons.

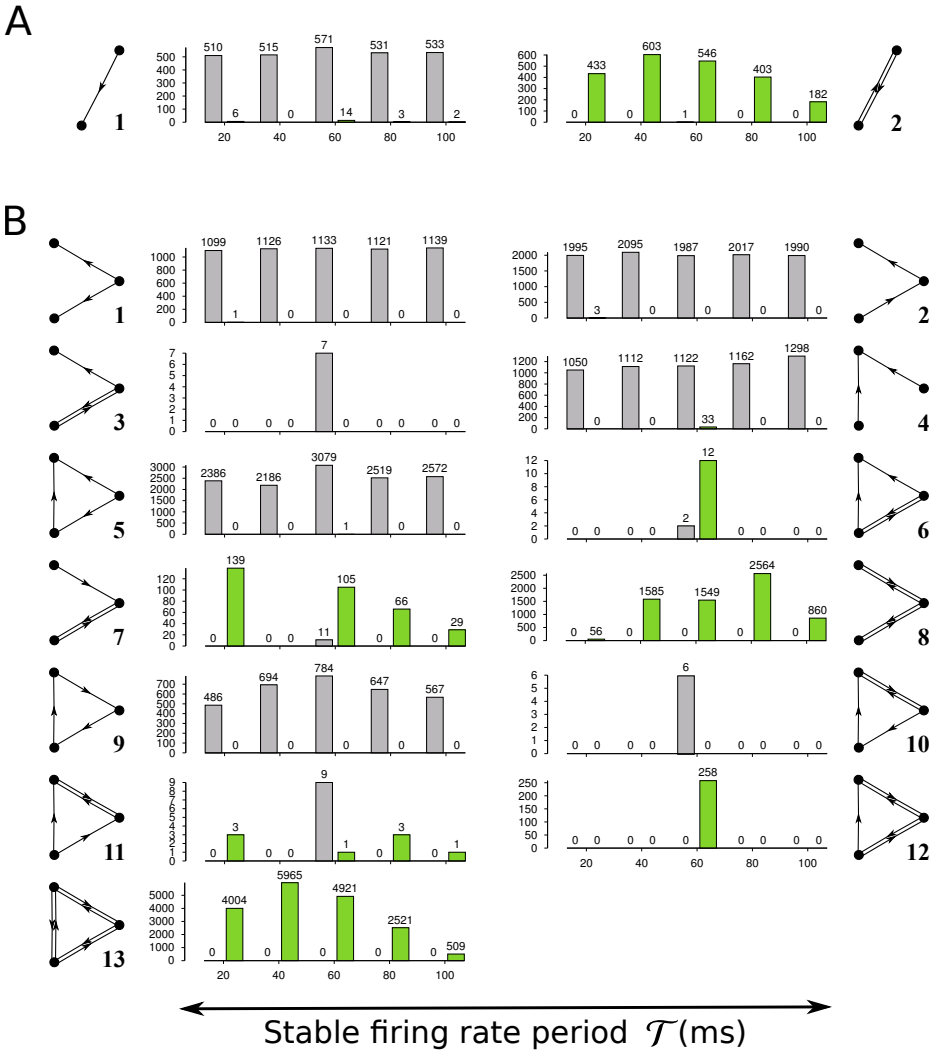

Figure 2: Synaptic connectivity in the recurrent network after the learning. (A) Two-neuron connectivity patterns. In each panel, horizontal and vertical axes are the duration $\mathcal{T}$ for which the firing rates of the Poisson neurons were stable and the frequency of the patterns. Forms of each connectivity pattern are indicated beside each panel. The corresponding ID is shown with the connectivity patterns. Gray and green bars are for standard and voltage-based STDP, respectively. The numbers above the bars show actual counts of the connectivity patterns.

ter the standard STDP learning (Fig. 2B, IDs 1, 2, 4, 5, 9). As well as these patterns, the patterns of combinations of bidirectional connections are only observed in the voltage-based STDP case. In our numerical simulation, it is difficult for both models to construct three-neuron connectivity patterns, that include both unidirectional and bidirectional connections in the network (Fig. 2 B, IDs 3, 6, 7, 10, 11, 12). From these results, it is suggested that the voltage-based STDP has a possibility to realize the statistics of synapses observed in the fine-scale cortical circuits [8, 9], if given connectivity to a network satisfies the anatomical statistics of synapses.

Next, we observed neuronal activities in two networks that were induced by the two different STDP rules. Neurons in the network sparsely fire and their activities are similar in both cases at first glance (Fig. 3 A). However, a frequency distribution of inter-spike intervals (ISIs) of the voltage-based model exhibits much different form from that of the standard model (Fig. 3 B). In the standard model case, neuronal firings are sparse and seem to be stochastic, and are observed in all the excitatory neurons (Fig. 3 A,C, left panels). On the other hand, in the voltage-based model, firings of some neurons in the network are localized and the other neurons do not fire as shown in Fig. 3 C, right panels.

Such differences of neuronal activities are derived from the different way of organization of strong feedforward connections. Organization of strong feedforward connections obviously differs between two models (Fig. 3 D). Although many of the feedforward connections are depressed by the standard STDP, all the excitatory neurons can obtain some strong connections (Fig. 3 D, left panel). The induction of stochastic neuronal firings (Fig. 3 C, left panels) is faithful to the organization of strong feedforward connections because many weak inputs and a few strong inputs

are injected to neurons in the network by random shifts of a center of the Gaussian profile. Strong unidirectional connections in the network emerges in accordance with these stochastic firings and an intrinsic property of the standard STDP [10].

When the voltage-based STDP is applied, strong feedforward connections are localized and some neurons fail to obtain strong feedforward connections (Fig. 3 D, right panel). The Gaussian profile locating at strong feedforward connections leads strong activations of neurons in the network, so that neurons behave as shown in Fig. 3 C, right-lower panel. In addition to the localization of the feedforward connections, the strong feedforward connections of some neurons locates at the same position (Fig. 3 D, right panel). For example, feedforward connections of the neurons 6, 7, 15, and 29 are strong at the same position. Then the localized firings of such neurons synchronously occur if the Gaussian profile meets the location of strong feedforward connections. The localized firings are efficient for the construction of strong bidirectional connections, not only between two neurons but also among three neurons, in the voltage-based STDP, because relatively high potentials of neurons last for the period where these neurons are activated. Consequently, the voltage-based STDP can lead lots of bidirectional connections in the network.

4. Conclusions

In this study we analyzed the properties of the voltage-based STDP model with respect to strong bidirectional connections. As a result, the voltage-based STDP model makes bidirectional connections strong not only between two neurons but also three neurons. Our results suggest that this novel model has a possibility to reproduce the statistics of synapses as observed in cortical circuits [8, 9]. The network discussed in this study had dense connections, however, synaptic connections among neurons are generally sparse but nonrandom connectivity [8, 9]. In addition, we did not consider the weight dependence of STDP in this study [5, 6, 18, 19]. Future work is to investigate the synaptic dynamics in the voltage-based STDP by introducing the condition described above.

Acknowledgement

The research is partially supported by Research Fellowships of JSPS (No. 22·8144) to HK. The authors would like to thank Dr. Kantaro Fujiwara for his valuable comments and discussions on this manuscript.

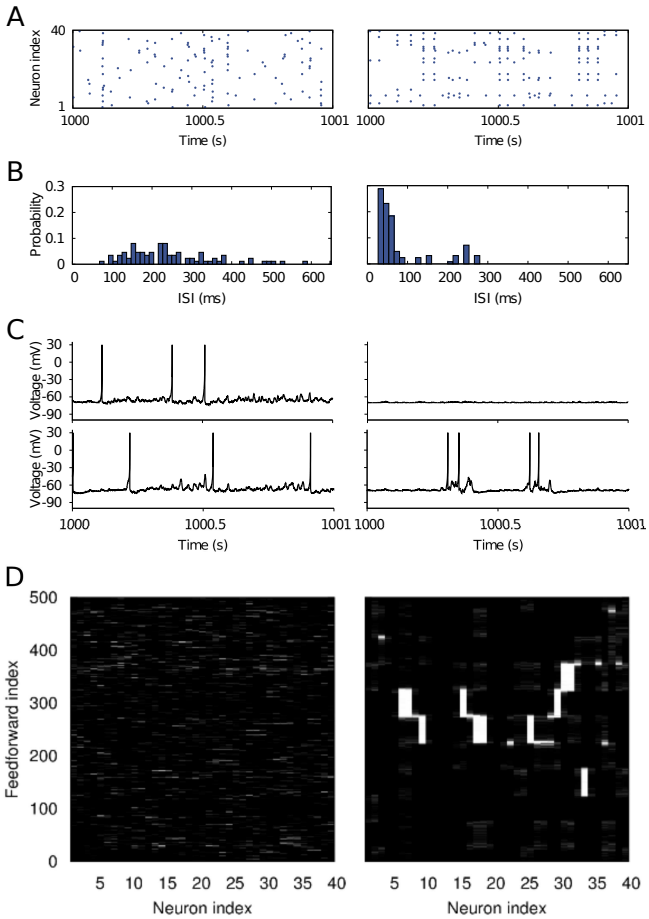

Figure 3: Neuronal activities and feedforward connections after the learning. (A) Rastergrams of excitatory neurons. (B) Frequency histograms of ISIs. These histograms were computed from (A). (C) Time courses of membrane potentials. Upper and lower panels correspond to neurons 1 and 6 in (A). (D) Feedforward connections organized by STDP. A horizontal axis represents the index of excitatory neurons in the recurrent network and a vertical axis represents the index of feedforward connections. The gray scale color represents synaptic weights. White and black correspond to the upper and lower bounds of feedforward connections.

References

[1] D. O. Hebb (1949), New York: Wiley.

[2] H Markram et al., (1997), *Science*, 275:213.

[3] G.-Q. Bi and M.-M. Poo (1998), *J. Neurosci.*, 18(24):10464.

[4] S. Song et al. (2000), *Nat. Neurosci.*, 3(9):919.

[5] M. C. W. van Rossum et al., (2000), *J. Neurosci.*, 20(23):8812.

[6] R. Gütig et al. (2003), *J. Neurosci.*, 23(9):3687.

[7] P. J. Sjöström et al. (2001), *Neuron*, 32:1149.

[8] S. Song et al. (2005), *PLoS Biol.*, 3(3):05070519.

[9] S. Lefort et al. (2009), *Neuron*, 61:301.

[10] S. Song and L. F. Abbott (2001), *Neuron*, 32:3390.

[11] C. Clopath et al. (2010), *Nat. Neurosci.*, 13:344.

[12] E. Schneidman et al. (2006), *Nature*, 440:1007.

[13] I. E. Ohiorhenuan et al. (2010), *Nature*, 466:617.

[14] R. Milo et al. (2002), *Science*, 298:824.

[15] E. M. Izhikevich (2003), *IEEE Trans. Neur. Net.*, 14(6):1569.

[16] S. Wernicke (2006), *IEEE/ACM Trans. Compt. Biol. Bioinfo.*, 3(4):347.

[17] C. Clopath and W. Gerstner (2010), *Front. Syna. Neurosci.*, 2(25):1.

[18] J. Rubin et al. (2001), *PRE*, 86(2):364.

[19] G. Hennequin et al. (2010), *Front. Compt. Neurosci.*, 4(143):1.